FEBS Letters 504 (2001) 152–160 FEBS 25153

Minireview

Inter-subunit rotation and elastic power transmission in F_0F_1-ATPase

Wolfgang Junge*, Oliver Pänke, Dmitry A. Cherepanov[1], Karin Gumbiowski, Martin Müller, Siegfried Engelbrecht

Division of Biophysics, University of Osnabrück, D-49069 Osnabrück, Germany

Received 11 July 2001; accepted 23 July 2001

First published online 8 August 2001

Edited by Andreas Engel and Giorgio Semenza

Abstract ATP synthase (F-ATPase) produces ATP at the expense of ion-motive force or vice versa. It is composed from two motor/generators, the ATPase (F_1) and the ion translocator (F_0), which both are rotary steppers. They are mechanically coupled by 360° rotary motion of subunits against each other. The rotor, subunits $\gamma\varepsilon c_{10-14}$, moves against the stator, $(\alpha\beta)_3\delta ab_2$. The enzyme copes with symmetry mismatch (C_3 versus C_{10-14}) between its two motors, and it operates robustly in chimeric constructs or with drastically modified subunits. We scrutinized whether an elastic power transmission accounts for these properties. We used the curvature of fluorescent actin filaments, attached to the rotating c ring, as a spring balance (flexural rigidity of $8{\cdot}10^{-26}$ N m^2) to gauge the angular profile of the output torque at F_0 during ATP hydrolysis by F_1. The large average output torque (56 pN nm) proved the absence of any slip. Angular variations of the torque were small, so that the output free energy of the loaded enzyme decayed almost linearly over the angular reaction coordinate. Considering the three-fold stepping and high activation barrier (>40 kJ/mol) of the driving motor (F_1) itself, the rather constant output torque seen by F_0 implied a soft elastic power transmission between F_1 and F_0. It is considered as essential, not only for the robust operation of this ubiquitous enzyme under symmetry mismatch, but also for a high turnover rate under load of the two counteracting and stepping motors/generators. **© 2001 Federation of European Biochemical Societies. Published by Elsevier Science B.V. All rights reserved.**

Key words: ATP synthase; F_0F_1; Motor protein; Actin; Elastic transmission

1. Introduction

Proteins operate as enzymes to catalyze and drive chemical syntheses, as ion pumps to generate electrochemical potential differences, and as motors to generate mechanical force. Among the mechano-enzymes, myosin, a linear motor stepping along actin filaments to contract striated muscle, the two-armed kinesin, walking hand-over-hand on microtubuli to pull synaptic vesicles along nerve axons, RNA polymerases, helicases and ribosomes, processing nucleotide strands, are all driven by nucleotide triphosphate hydrolysis. The rotary flagellar motor which propels bacteria, on the other hand, is powered by an electrochemical potential difference across the cytoplasmic membrane. ATP synthase is a mechanical enzyme which can use both types of driving forces for intra-protein rotary motion. It produces ATP at the expense of an electrochemical potential difference or, when operating in reverse, it generates an electrochemical potential difference at the expense of ATP hydrolysis (then called F-ATPase).

For decades it has remained enigmatic how the two functions, the electrochemical and the chemical one, are linked with each other. They are rather well separated in the bipartite structure of the enzyme, with its ion-conducting membrane portion, F_0, and the peripheral F_1 portion, which without F_0 only can hydrolyze ATP. It is now established that ion transport and ATP synthesis by the holoenzyme are mechanically coupled. The holoenzyme consists of two rotary motors that are mounted on a central shaft and kept together by an eccentric connection (Fig. 1A). Depending on the demand for ATP or for ion-motive force, one motor operates in the forward direction, and, by rotating the central shaft, drives the other motor backwards to operate as a generator. Of the same size as myosin and by an order of magnitude smaller than the flagellar motor, ATP synthase presents a delicate blend of electrochemical-to-mechanical-to-chemical energy conversion (for reviews see e.g. [1–6]. Its at least eight different types of subunits (*Escherichia coli* nomenclature) are attributed either to F_1 ($\alpha_3\beta_3\gamma\delta\varepsilon$) and F_0 ($\mathbf{ab_2c}_{10-14?}$), or they are grouped into the 'rotor' ($\mathbf{c}_{10-14?}\gamma\varepsilon$) and the 'stator' ($\mathbf{ab_2}\delta(\alpha\beta)_3$). The designations of 'rotor' and 'stator' are relative, since the enzyme carries out rapid rotational (Brownian) diffusion within the membrane at correlation times of 100–200 μs [7,8].

The molecular design of this twin engine comprises two surprising features, (1) the symmetry mismatch between F_0 and F_1 and (2) an astounding robustness of the function against alterations of the mechanical properties of the protein subunits. The latter is especially evident in chimeric enzyme constructs from different organisms and in mutant enzymes with substantially modified subunits – shortened, stiffened, cross-linked – without affecting the functions like the inter-subunit rotation altogether.

In this article we address how an elastic power transmission between the two motors/generators might cope with the symmetry mismatch, and how it might overcome restrictions as imposed by chimeric constructs or functionally impaired subunits. The argument necessitates a digression into techniques to detect the rotation in the holoenzyme, and into the visco-elastic properties of actin filaments which can be used as a

*Corresponding author. Fax: (49)-541-969 2262.
E-mail address: junge@uos.de (W. Junge).

[1] Permanent address: Frumkin Institute of Electrochemistry, Moscow, Russia.

0014-5793/01/$20.00 © 2001 Federation of European Biochemical Societies. Published by Elsevier Science B.V. All rights reserved.
PII: S0014-5793(01)02745-4

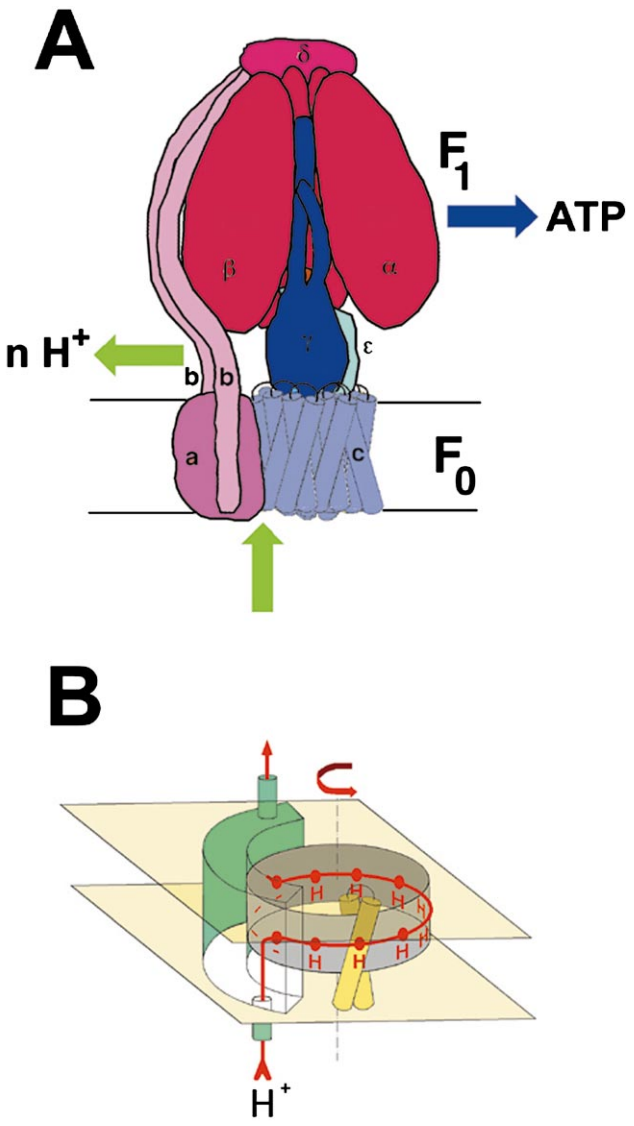

Fig. 1. A: F_0F_1: two stepping motors/generators mounted on a common rotary shaft. 'Rotor' subunits are blueish, 'stator' subunits reddish. B: One possibility for a construction principle of the ionic drive F_0 [5].

spring balance to gauge the angular torque profile of the enzyme.

2. The symmetry mismatch between F_0 and F_1

Both elements of this twin rotary engine, F_0 and F_1, are steppers. There are three catalytic sites on F_1. They are equivalent in the time average, but structurally [9] and functionally [10] they differ at any moment. The functional state rotates during turnover.

The three-stepped rotary progression of subunit γ during ATP hydrolysis has been inferred from polarized photobleaching absorption recovery with a single chromophore on subunit γ [11,12], from the polarized fluorescence of such a probe [13], and recently directly resolved at high quality by dark-field microscopy [14]. A 40 nm gold particle served as a probe on subunit γ. At low ATP concentrations (some 1 μM) Yasuda et al. resolved 90° and 30° substeps which were attributed to ATP binding and ADP release, respectively. At high concentrations of ATP the 3+3 steps merged into three steps. From previous work it was known that the resting positions of the stepping and load-free F_1 are separated by Arrhenius activation energies of between 40 and 50 kJ/mol [15]. At very low ATP concentrations (some 10 nM) the three-stepped progression has been resolved in micro-videography with a fluorescent actin filament attached to subunit γ [16]. The enzyme turnover was then very low and (diffusion-)controlled by the supply of the substrate rather than by the viscous load on the filament. Taken together these results have revealed the F_1 portion of the enzyme as a three-stepped rotary engine.

The step number of the other engine, F_0, is under contention. A prominent portion of the rotor part of F_0 is a ring of N identical copies of subunit **c**. If the enzyme is tightly coupled and in the absence of slip between the two motors, the translocation of N ions has to be matched to the synthesis/hydrolysis of three molecules of ATP. There is evidence that the copy number, N, of subunit **c** in the ring varies between different organisms. In *E. coli* it has been inferred from cross-linking studies that the enzyme can work with $N = 12$ copies [17]. In chloroplasts, functional studies on the proton-over-ATP stoichiometry both under static head conditions [18,19] and far from thermodynamic equilibrium [20] have yielded a number of four protons translocated per ATP synthesized, and this has also pointed to a stoichiometry of 12 monomers of subunit **c** on the ring-shaped oligomer.

Recently, structural studies produced different numbers of monomers on **c** rings. The crystal structure of the yeast enzyme revealed $N = 10$ [21]. It has remained an open question, though, whether or not the lack of subunits **a** and **b** in the crystals was accompanied by loss of some copies of the equivalent of subunit **c**. $N = 14$ was obtained by atomic force microscopy with two-dimensional crystals of the **c** ring oligomer from chloroplasts [22]. The high copy number might have, however, resulted from a rearrangement of subunit **c** under the conditions of two-dimensional crystallization. Perhaps the most convincing example of a stoichiometry deviating from previous expectation is $N = 11$ as recently shown (also by atomic force microscopy) for isolated **c** ring oligomers from *Ilyobacter tartaricus* [23]. This oligomer is extremely stable in detergent and requires autoclaving for dissociation which would render a rearrangement during crystallization unlikely. Whether the copy number in the **c** ring is fixed for any given organism, or even flexible and depending on the physiological conditions, is an interesting open question. It would introduce a gear-shift between the two motors/generators.

One possible construction principle of the ionic drive is illustrated in Fig. 1B. It is based upon rotational fluctuations of the **c** ring relative to the large subunit **a** (shown in green) and on certain electrostatic constraints which have been detailed elsewhere [24,25]. The general validity for all organisms of this two-channel model has been questioned and a one-channel model has been proposed, instead (reviewed in [26]). It has been discussed elsewhere [27] that the two alternatives are equivalent with respect to their dynamic behavior. The open controversy thus does not bear on the stepped nature of the ionic drive, which is the topic of this article.

Taken together the above described results have revealed the F_0 portion of the enzyme as a 10–14-stepped rotary engine.

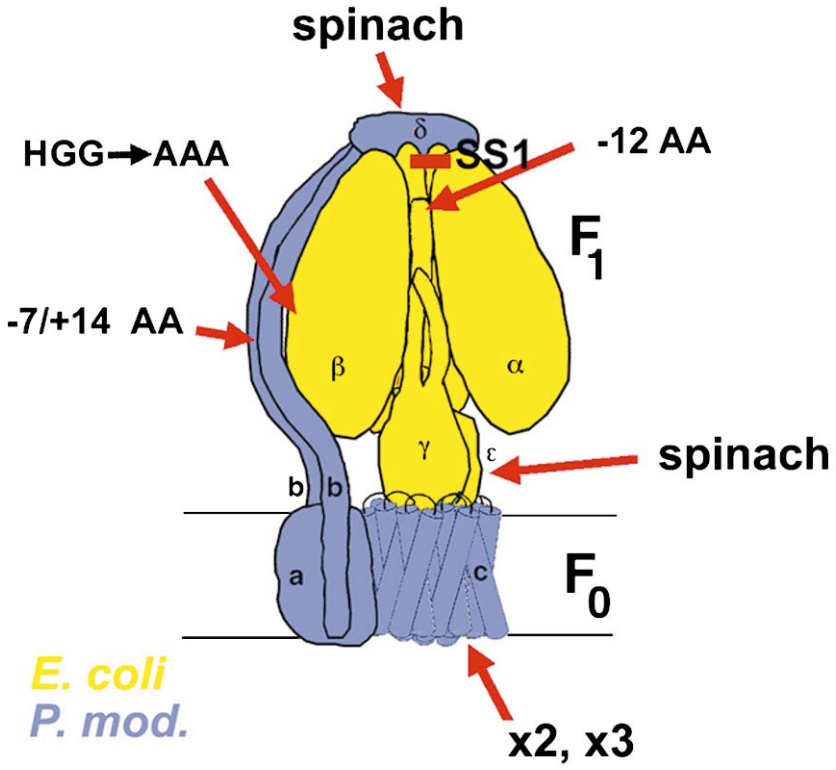

Fig. 2. Chimeric and structurally impaired but functional constructs of F_0F_1. The astounding functional robustness of the enzyme (see text for details).

3. Chimeric and structurally impaired but functional constructs of F_0F_1

Chimeras composed from subunits of evolutionary remote organisms, and likewise some enzyme constructs with severely altered subunits have been found to retain their function (Fig. 2). In mutants of the *E. coli* enzyme where certain subunits had been deleted, cell growth on succinate could be restored by complementation with cyanobacterial subunits α, β, or with cyanobacterial or spinach chloroplast subunits δ and ε (labeled 'spinach' in Fig. 2) [28]. A chimeric spinach chloroplast subunit β containing the respective *E. coli* sequence for residues 1–96 could substitute for *E. coli* β [29]. Likewise, cyanobacterial subunits δ and ε could substitute for their *E. coli* counterparts [30]. These results are surprising for two reasons: (i) the binding strength of subunit δ to $(\alpha\beta)_3$ has to be very high (in the chloroplast enzyme is very high, indeed ($\Delta G^\circ > 52$ kJ/mol [31])). (ii) The primary structures of both δ and ε are among the least conserved in F-ATPases. Still the interface contacts between subunits seem to be compatible among different organisms so that they withstand the high torque of this twin engine (see below). Even more dramatic examples for the robustness of this enzyme include the following. The F_0 portion of *Propionigenium modestum* which is designed to operate with sodium ions rather than protons can functionally replace its 'proton-conducting counterpart' from *E. coli*. The chimeric enzyme, consisting of subunits **a**, **b**, **c**, and δ from *P. modestum* and α, β, γ and ε from *E. coli* (color coded accordingly in Fig. 2), can operate with both, protons and sodium ions, depending on their concentrations [32,33]. In the same line, enzymes with structurally altered subunits proved to retain function. The supposedly long and stretched subunits **b** of the *E. coli* enzyme are expected to be largely α-helical [34,35]. These subunits are part of the 'stator'. Surprisingly, **b** could not only be lengthened by 14 residues [9] (which might have simply caused an 'outlooping' of single turns [36]) but also shortened by up to seven residues ('−7/+14 AA' in Fig. 2) [37], i.e. by nearly two turns and stretching the remainder by about 8%, without affecting the function. Amino acid sequences which are highly conserved can be changed or deleted altogether. An example for the first is the *E. coli* β_{D380C} mutation [38], for the latter the deletion of the α-helical part of subunit ε or the last 10 residues of *E. coli* γ [39]. Recently, we deleted up to 12 amino acids at the C-terminus of subunit γ without complete loss of function ('−12 AA' in Fig. 2, M. Müller et al., unpublished). This stretch is the very portion of the rotary rod supposed to snugly fit into the hydrophobic bearing in $(\alpha\beta)_3$. Yoshida's group has point-mutated residues in the hinge region of subunit β essential for opening and closing the active site ($\beta_{H179A/G180A/G181A}$, 'HGG→AAA' in Fig. 2) [40]. Although this abolished the ATPase activity by 99% it did not prevent the rotation of γ, and it did not even change the magnitude of the torque. Whereas Cross's group found that a disulfide bridge between subunits β and γ inhibited the activity if placed at the lower part of F_1 ($\beta_{D380C} \leftrightarrow \gamma_{C87}$, 'SS3') [38], which we reproduced and extended to the center of F_1 ($\alpha_{A334C} \leftrightarrow \gamma_{L262C}$), we found that cross-linking the 'tip' of γ (i.e. the penultimate C-terminal residue) with its neighbor residing in subunit α, namely $\alpha_{P280C} \leftrightarrow \gamma_{A285C}$ (see Fig. 2), left both ATP hydrolysis and rotation completely unaffected (K. Gumbiowski, M. Müller and O. Pänke, unpublished). This may be explained by the forced rotation around the dihedral angles of some of the residues in that region of γ although the complete lack of

effect could raise the assumption that this very part of γ never rotates at all, even not in the wild type enzyme. Finally, Fillingame's group has shown that subunit **c** can be genetically fused to $\mathbf{c}_2$ dimers or $\mathbf{c}_3$ trimers [41] without affecting its function dramatically (labeled '×2, ×3' in Fig. 2).

Taken together the cited results demonstrate that the enzyme operates astoundingly robust if exposed to severe structural modifications.

4. Inter-subunit rotation in the holoenzyme, F_0F_1

In the isolated and immobilized F_1 portion the rotation of subunit γ relative to $(\alpha\beta)_3$ has been unequivocally demonstrated by micro-videography. A fluorescent actin filament of μm length, attached to subunit γ, served as a reporter [42] (other methods included chemical cross-linking [38] and polarized photometry [43]).

That the rotary function extends into F_0 has been first inferred from numerous cross-linking experiments carried out mainly by Capaldi's lab. In a recent paper [44], by combining cross-links that were engineered and described previously, it was shown that disulfide-bridging the putative rotor subunits γ, ε, and **c** of EF_0EF_1 did neither affect ATP hydrolysis, nor proton translocation, nor ATP synthesis. These activities were, however, obtained without direct demonstration of rotation.

It seemed straightforward to extend the micro-videographic technique to the holoenzyme. It has not yet been feasible, however, to use this assay with the fully functional and membrane-embedded F_0F_1. The detergent-solubilized enzyme, on the other hand, apparently lost the coupling of ATP hydrolysis to proton translocation. These complications and their solution are reviewed in the following.

The first report of a rotating **c** ring in isolated EF_0EF_1 upon ATP hydrolysis was published by Futai's group [45]. They used an approach similar to the one originally introduced for F_1 by Noji et al. [46]. The enzyme was immobilized via His-tags engineered into the N-termini of subunit α. A fluorescent actin filament was attached via streptavidin to biotinylated subunit **c**. This necessitated a point mutation of subunit **c** in order to introduce the required Cys residue as attachment point for biotin-maleimide. The rotation was weakly venturicidin sensitive, DCCD insensitive, and the yield of rotating filaments was low (0.4%, but still significant in single molecule studies). The conclusiveness of this work was immediately criticized [47,48] based on two arguments: (1) the DCCD insensitivity might indicate an uncoupled enzyme which either lacked subunits **a** and **b** of EF_0 altogether (as observed with the crystallized yeast F_0F_1 [21]) or contained them in a 'disordered' and decoupled manner, so that the rotation of the ring was no longer coupled to proton transfer. (2) The low yield was interpreted to indicate mislabeling. If this had occurred at a Lys residue on γ of F_1 (due to some residual reactivity of maleimide for Lys) the observed rotation in F_1 was just confirmatory. The possibility of mis-derivatization was overcome by our own work [49]. We used a Cys-free mutant of EF_0EF_1 [50] with a genetically engineered Strep-tag attached to the C-terminus of each subunit **c**. This allowed for specific attachment of biotinylated actin filaments via the streptavidin derivative streptactin. Immobilization of EF_0EF_1 was via His-tags engineered into the N-termini of subunits β [51]. With this approach the yield of rotating filaments was raised by more than one order of magnitude up to 5% (cf. Fig. 3 in [49]). The DCCD issue was not solved since the use of detergent for the solubilization of EF_0EF_1 was unavoidable. We tried to address it by using DCCD-pretreated EF_0EF_1

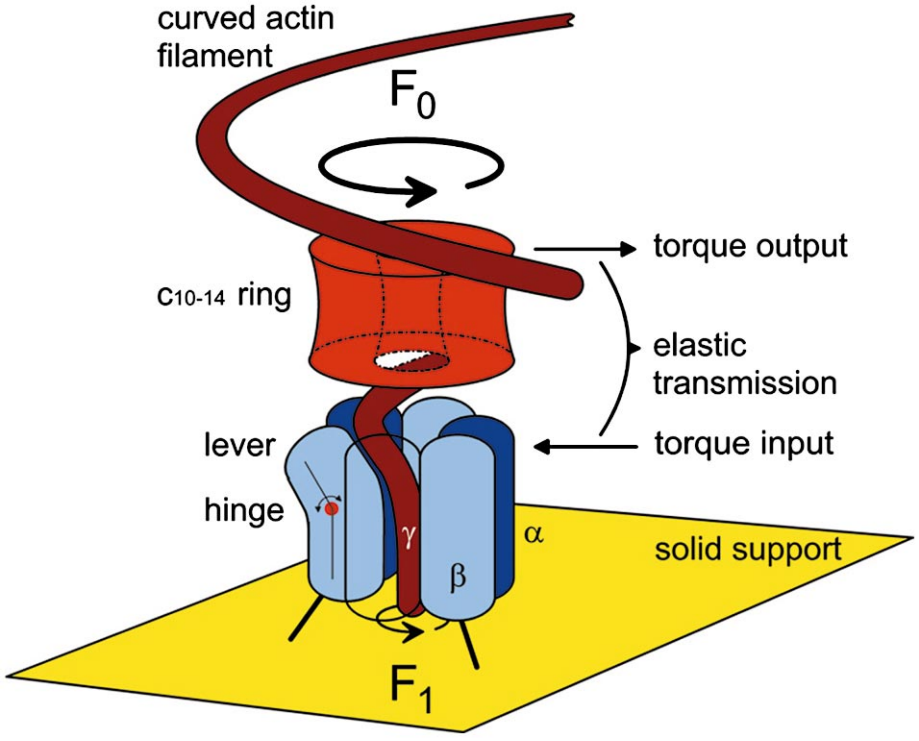

Fig. 3. The rotational assay for the **c** ring in immobilized and detergent-solubilized F_0F_1 (see text for details and [54]).

and compared the relative occurrence of rotating filaments in the rotation assay in the presence of detergent and after washing it away after immobilization of EF_0EF_1. The results qualitatively agreed with expectation, i.e. the number of rotating filaments in DCCD-pretreated samples was lower than in untreated controls (K. Gumbiowski, unpublished observations). However, because this number decreased further after washing, the result was not conclusive. In another approach we used the EF_0 mutant $\mathbf{c}_{D61N}$, which is known to have lost the capability to synthesize ATP since it lacks the essential Asp_{61} [52]. This mutant produced rotating filaments just as the control (K. Gumbiowski and O. Pänke, unpublished data). Taken together these data imply that detergent-solubilized EF_0EF_1 is decoupled at its ion-motive portion, although all subunits are present. Still ATP hydrolysis causes subunits γ, ε and the ring of $\mathbf{c}_N$ to corotate. A similar observation was reported by Fillingame's group showing that mutations in the second or third loop of genetically fused subunits **c** left the enzyme fully functional just as wild type $\mathbf{c}_2$ dimers or $\mathbf{c}_3$ trimers [41]. In another approach Futai's group immobilized the 'rotor' via His-tagged subunits **c**, and demonstrated rotation of the 'stator' by attaching fluorescent actin filaments to biotin-tagged subunits α and β [53]. We obtained the same result with the His-tag/Strep-tag approach (O. Pänke and K. Gumbiowski, unpublished). All in all, there would be but little doubt about the expected rotation of subunits $\gamma\varepsilon\mathbf{c}_{10-14}$ relative to $(\alpha\beta)_3\delta\mathbf{ab}_2$, both in ATP hydrolysis and synthesis. To satisfy purist's requirements, however, we are still lacking visual demonstration of rotation in appropriately immobilized F_0F_1 and powered by ion-motive force.

5. The viscoelastic properties of an actin filament fixed to the rotation axis of the enzyme

The rotation of subunit γ relative to $(\alpha\beta)_3$ driven by the hydrolysis of ATP has been unequivocally demonstrated by micro-videography, with a fluorescent actin filament of μm length attached to γ and immobilizing the enzyme via His-tagged β [42]. Whereas the rate of ATP hydrolysis by isolated and load-free F_1 approaches 300 s^{-1} (equivalent to 100 revolutions per second), the viscous drag on the rotating filament (which is 200–300 times longer than F_0F_1!) lowered the rotational rate of actin-loaded F_1 by four orders of magnitude down to 0.1 s^{-1}. Not unexpectedly, details of the rotary motion were blurred by the strong viscous damping.

Taking the three-fold stepping of the F_1 motor as granted, we asked for the torque profile as delivered to the ion-motive device, in particular to the **c** ring of F_0. The key question was whether or not the intrinsic stepping of F_1 was smoothed in order not to interfere with the different stepping in F_0.

In the experiments we used the same protocol as given in Section 4, namely a detergent-solubilized F_0F_1 that was immobilized on a solid support via N-terminal His-tags attached to subunits β. A Strep-tag affinity peptide was engineered into the C-terminal end of each copy of subunit **c**, and a fluorescent actin filament was linked via the Strep-tag/streptactin/biotin linkage to the **c** ring. The construct is illustrated in Fig. 3 (for experimental details, see [54]). As a new approach we gauged the torque profile by the curvature of the enzyme-attached filament instead of by its rotation velocity as in previous work [55,56]. The rotation velocity in fact is a poor indicator of the torque. One example, if the filament contacts an obstacle on the surface, the velocity becomes zero despite of the persisting torque. Under the same conditions, however, the filament is still curved in proportion to the enzyme-generated torque. This prompted us to use the filament as an elastic spring balance, evaluating its compliance at any angular position to yield the torque profile. This approach is strictly valid if the rotation is fully stalled, its application to the moving enzyme has required a thorough theoretical analysis of the viscoelastic dynamics of the enzyme/filament construct [57]. The results are summarized in the following.

Let us consider an actin cantilever which is fixed at one end of the rotation axis of the enzyme and free at the other. As the cantilever is moving at a very low Reynolds number, its fine structure and the detailed shape of the surface are 'effectively

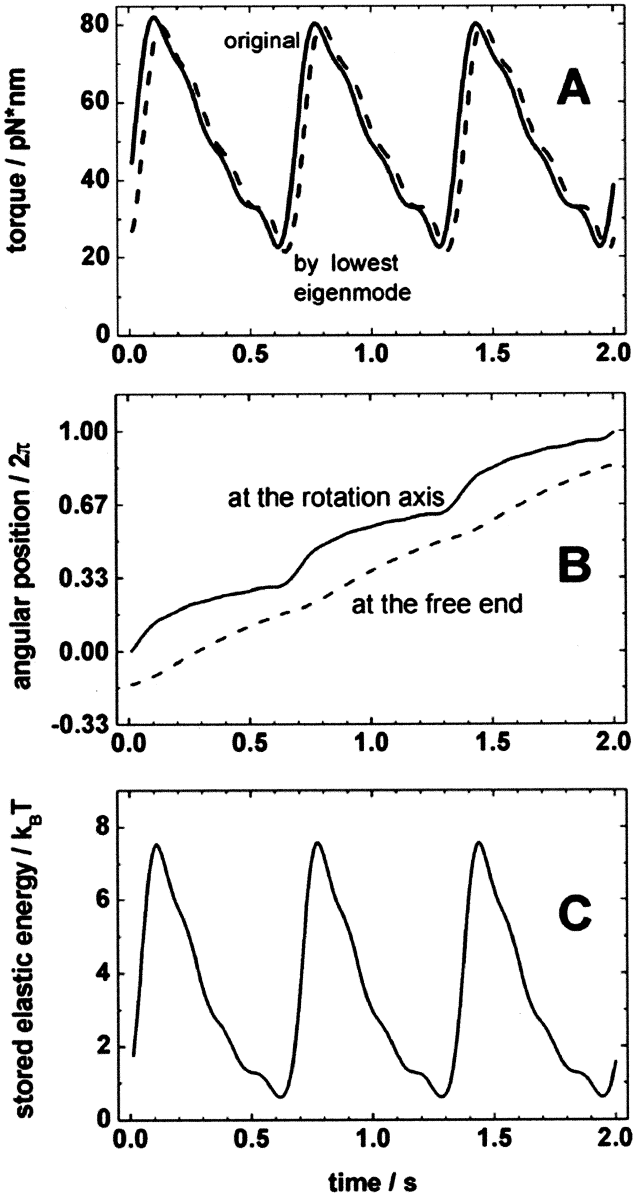

Fig. 4. Simulated behavior of a rotating actin cantilever. A: Assumed torque profile of the driving rotor as a function of time. B: Progression at the axis (top curve) and at the free end (lower curve). C: Elastic energy stored by the actin filament in units of k_BT [57].

smoothed by the viscous fluid' (weak, i.e. logarithmic dependence of the friction coefficient on the width/length ratio). It can be considered as a cylindrical rod (diameter 5.6 nm, typical length 3 μm). Following common practice in mechanics, the dynamic behavior of F-actin is described in terms of so-called orthonormal eigen modes. Because, in this regime, the viscous drag in the fluid is much greater than the small inertial force of the filament [58], the dynamic behavior of the filament is over-damped, 'relaxation instead of oscillation'. The spatial shapes of these modes resemble the familiar ones of an oscillating cantilever with n ($n = 0, 1, 2, 3,...$) nodes over the length excluding the ends. A simulation of the dynamic behavior of rotating actin filaments using realistic parameters has shown that the fundamental normal mode with the longest relaxation time (typical 140 ms) dominates the behavior in the time range of some 10 ms, whereas the relative extents of the next three higher modes are about 40, 300, 1100 times smaller and about 40, 300, 1100 times more rapidly damped away. As intuitively expected, the slow response of the lowest mode blurs details of the enzyme's internal rotary motion. On the other hand, the momentary curvature at the rotational axis is almost proportional to the torque at any given angular position. This feature has not been exploited until now. The seeming disadvantage of the slow viscoelastic relaxation thus can be turned into a useful tool [57]. Fig. 4B illustrates the simulated angular progression of a rotating actin filament at the axis (structured) and at the free end (highly damped) under the influence of the torque profile which is illustrated in Fig. 4A. During revolution the filament transiently stores and dispenses elastic energy in the order of 8 k_BT units (k_B is the Boltzmann constant) as given in Fig. 4C. It should be noted here that the standard free energy of ATP hydrolysis, −30 kJ/mol, amounts to 12.5 k_BT.

In summary, an actin filament which is attached to the rotor portion is a valuable indicator of the torque only through its curvature, which exists both during movement and during halts caused by surface obstacles.

The above considerations have been based on an idealized situation, an actin filament driven at its fixed end by the rotary enzyme and moving in a homogeneous viscous fluid. In the realm of typical experiments, however, a filament of 3 μm length and less than 10 nm radius moves a few 10 nm high over a rough surface of a protein-covered solid support. Not only that the viscosity close to the surface is greater than in the bulk [59], but contacts with the surface may increase the apparent friction or even obstruct the motion. In an attempt to extend the validity of the above described idealized concept we have calculated the curvature of actin filaments at constant torque as a function of three different distributions of the compensating force over length. The calculated curvature was only little dependent on whether the force distribution was linear (viscous drag), constant (surface friction) or concentrated (obstacle contact). Broadly speaking, the idealized approach is applicable to any typical experimental situation [57].

Evaluation of data on fluctuating and rotating actin cantilevers fixed to the **c** ring of EF_0EF_1 [60] eventually yielded (a) Young's modulus of elasticity of F-actin and (b) the torque profile of the chemical drive of F_0F_1 as a function of the angular reaction coordinate. These results are summarized in the following.

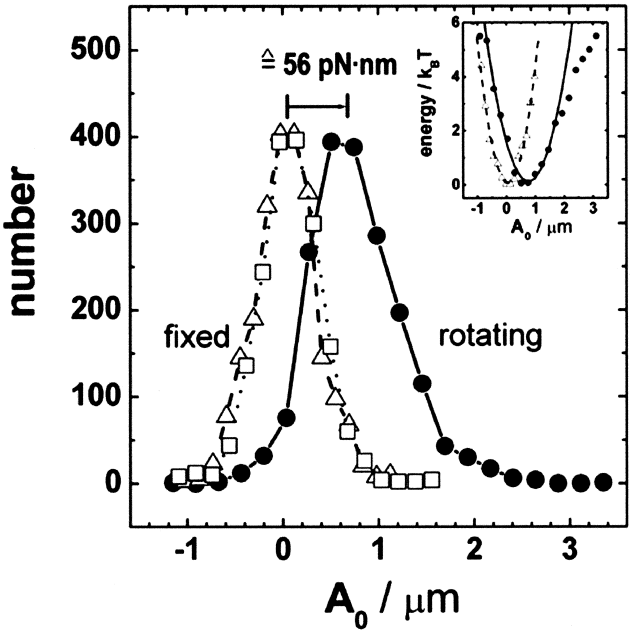

Fig. 5. Histograms of the maximal end-displacements of a rotating (length 2.6 μm, circles and solid line) and a non-rotating and just fluctuating filament (length 2.0 μm, open triangles and broken line). The shift of the peak position of rotating filament implies an average torque of 56 pN nm. The insert shows logarithmic replots of the data points and a parabolic approximation to the energy profile of the elastically deformed actin cantilevers [60].

6. The smoothing of the output torque by an elastic power transmission between F_0 and F_1

Under physiological conditions, in photosynthetic and respiring organisms, the torque which is generated by proton flow through the F_0 motor operates against the counter-torque, which is generated by ATP hydrolysis in F_1. Under static head conditions, eventually, the two torques are balanced, and the enzyme rests in a state of dynamic equilibrium. When operating close to this state, it may run very slowly under thermodynamic control. In this case the two motors operate against each other thereby elastically straining the two portions of the enzyme, stator and rotor. The situation is very different if one motor/generator is removed, then the remaining one runs freely under kinetic control.

We studied the operation of a F_0F_1 construct in a situation very close to thermodynamic control. The torque was provided by ATP hydrolysis and the counter-torque was delivered to the **c** ring of F_0 by the elastic deformation of an attached actin filament that experienced viscous drag, friction or obstacles [60]. Insofar, our study relates to a model system. Regrettably, the fully coupled enzyme, with proton-motive counter-torque, has so far withstood this approach for technical reasons.

In our hands, the common approach to estimate the average torque from the average rotation rate of the actin filaments and assuming that the filament felt the viscosity of the bulk medium yielded too low torque values compared with the expected figure for a non-slipping rotary enzyme. We have obtained figures of the apparent torque ranging between 20 and 30 pN nm. This torque times the angular progression, i.e. $2\pi/3 = 2.094$ per ATP molecule hydrolyzed, gives the apparent

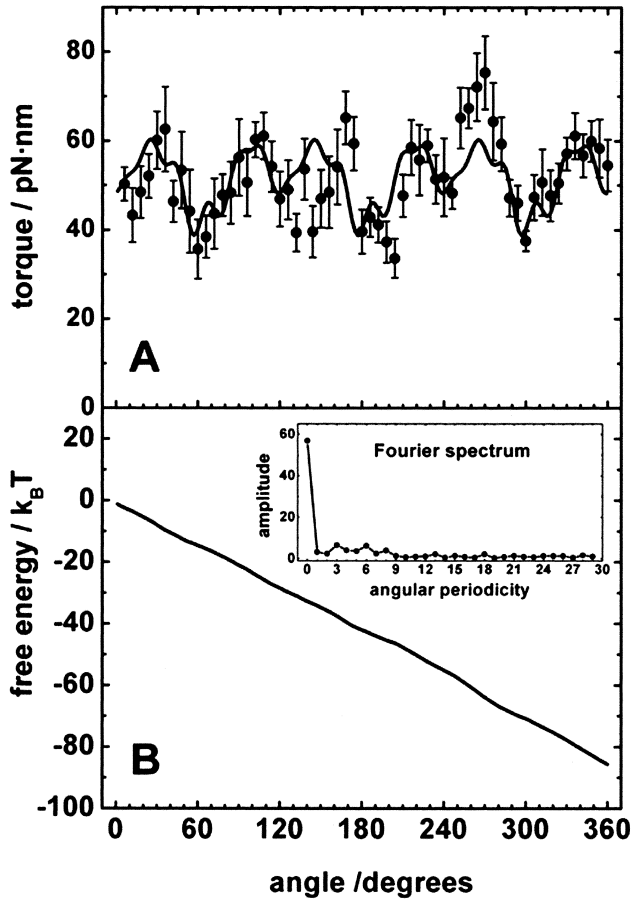

Fig. 6. The angular dependence of the average output torque (A) and the respective free energy profile (B) of the F_0F_1 construct. This profile was calculated from more than 20 turnovers for each of six rotating filaments with the working length ranging between 1.4 and 2.6 μm. The insert shows the Fourier spectrum of the experimental points from the top panel (circles). The smooth curve on the top panel was obtained as a filtered back-transform of the Fourier spectrum. It represents an idealized angular dependence of the torque under the assumption of a three-fold symmetry of the torque generator and thereby differs from an unbiased fit to the data [60].

free energy change at the output. It amounts to 42 and 63 pN nm or 25 and 38 kJ/mol, respectively, which is essentially smaller than the free energy of ATP hydrolysis under the given experimental conditions which amounts to around 65 kJ/mol. This has qualified previous conclusions as to a perfect, non-slipping operation between ATP hydrolysis in F_1 and torque generation [61,62].

The alternative approach, to gauge the torque by the elastic deformation of actin filaments, as theoretically outlined in [57] has produced a greater figure for the average torque, namely 56 pN nm [60]. The flexural rigidity of the actin filaments, which were used as a spring balance, is a crucial parameter in these experiments. The rigidity was determined from bending thermal fluctuations both of rotating and non-rotating filaments. Fig. 5 shows histograms of the deflection of the free ends of a rotating and a fixed actin filament. The different width of the respective profiles is attributable to the different length of these particular filaments. In both cases, the width implied a flexural rigidity of F-actin, namely $8.2 \pm 3.0 \cdot 10^{-26}$ N m^2, that is consistent with the previously published findings based on the analysis of bending fluctuations of unconstrained filaments [63,64] and twisting fluctuations of an immobilized and stretched F-actin filaments [65,66]. The difference between the central positions of the rotating and the non-rotating filament is proportional to the average torque generated by the enzyme. Its magnitude, 56 pN nm, which is 1.5–2.5 times greater than obtained by the common technique [54,67–69], agreed reasonably well with the expected figure based on thermodynamic control in a perfectly coupled ATPase. It has proven the absence of slip between ATP hydrolysis and torque production in F_1F_0-ATPase.

Using the curvature of elastically deformed and rotating filaments at different angular positions and averaging it over many rotary runs through any position we have calculated the torque profile of F_1F_0 molecules as a function of the angular displacement. Precise measurements of the torque profile as a function of the angular position are essential for understanding the role of the partial reactions (ATP binding, hydrolysis, product release) in the torque generation. By digital image analysis of long rotary trajectories and Fourier analysis we have found a relatively smooth angular dependence of the torque that varied in the range of 30–80 pN nm (see Fig.

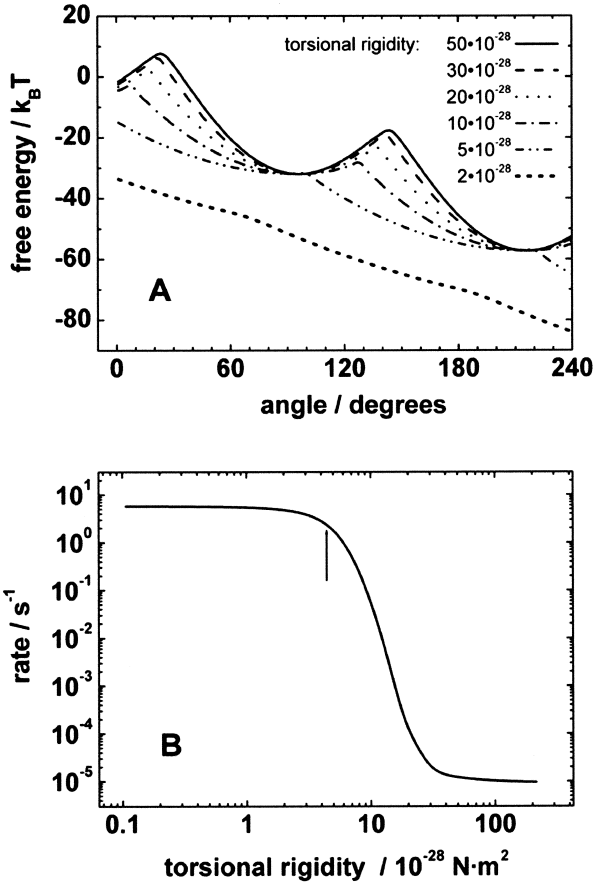

Fig. 7. A: Simulation of the angular free energy profile of a C3 symmetrical rotary engine with elastic power transmission under variation of the torsional rigidity. The angular dependence of the output free energy strictly reproduces the internal one in the case of an inflexible transmission (the solid line). A soft transmission, however, smoothes the output profile (broken lines were calculated for decreasing torsional rigidity in N m^2 as indicated). B: The calculated rotation rate of this motor (average torque 56 pN nm) when loaded by an actin filament moving in a viscous medium. The arrow indicates the probable torsional rigidity of the enzyme/filament construct [60].

6A). The angular dependence had small periods of three and six peaks and troughs over 2π, but their contributions in the Fourier spectrum were by order of magnitude smaller than the extent of the constant component, and hardly discernible from noise.

Integration of the output torque over the angular domain yielded the standard free energy at the output of the enzyme. Its rather linear and featureless angular dependence (see Fig. 6B) is consistent with the concept of an elastic power transmission between the inner chemical motor in F_1 (the contact sites between subunits $(\alpha\beta)_3$ and γ) and the driving machinery of proton transfer (the ring of **c** subunits). This is detailed in the following.

ATP hydrolysis by load-free F_1 is three-stepped with activation barriers greater than 40 kJ/mol as cited above. The load-free enzyme is expected to run up and down the valleys and hills of its free energy profile as illustrated by the solid line in Fig. 7. Its rate of progression depends, by the Eyring-Polanyi (Arrhenius) argument, on thermal input to cross the activation barrier. If such a motor is rigidly coupled to a μm long actin filament its motion is drastically slowed by the viscous drag of the long filament. In the case of a rigid transmission between F_1 and the actin filament the average curvature of the latter (output) is proportional to the first derivative of the internal free energy profile of F_1 (input). An elastic transmission flattens the output dependence. We have treated this situation by application of the Langevin equation and obtained the simulated behavior [60] that is depicted in Fig. 7. Fig. 7A shows the simulated output free energy profile as a function of the rotation angle of a stepping motor which is coupled to an actin filament in viscous fluid with the elastic modulus of an elastic power transmission as a parameter. It is obvious that the profile is the smoother the softer the elastic power transmission. The rationale for the smoothing of the output energy profile is the transient elastic storage of energy during the falling segment of the reaction path and its utilization during the rising segment. One important consequence of the smoothed free energy profile is that it allows for greater speed of this machine under load. Fig. 7B shows the calculated turnover rate of the coupled device as a function of the torsional rigidity of this transmission. It is apparent that stiffening the transmission results in lowering of the rate. These considerations have been derived based on the experiments with the holoenzyme under somewhat artificial conditions where the intrinsic counter-torque by the ion-motive motor F_0 is replaced by the one of an actin filament. It is obvious, however, that these considerations can be transposed to the natural operation of the enzyme, when the two motors/generators work against each other.

The elastic power transmission is considered as important, (1) for the robust operation of this ubiquitous enzyme under symmetry mismatch (C_3 versus C_{10-14}), and (2) for high turnover rate of the two counteracting and stepping motors/generators in ATP synthase. The internal elasticity might also provide a clue to the remarkable functional robustness of this enzyme. The molecular basis for the elastic elements, involving both the stator and the rotor portions, still has to be characterized.

Acknowledgements: The authors thank H. Kenneweg and G. Hikade for excellent technical assistance. This work was financially supported by Grants from the Deutsche Forschungsgemeinschaft (SFB 431/D1 to W.J. and S.E.), the Human Science Frontier Program (RG 15/1998-M to W.J.), the Fonds der chemischen Industrie, and the Land Niedersachsen, and by an Alexander von Humboldt Fellowship to D.A.C.

References

[1] Leslie, A.G., Abrahams, J.P., Braig, K., Lutter, R., Menz, R.I., Orriss, G.L., van Raaij, M.J. and Walker, J.E. (1999) Biochem. Soc. Trans. 27, 37–42.
[2] Oster, G. and Wang, H. (1999) Structure 7, R67–R72.
[3] Kinosita, K., Yasuda, R., Noji, H., Ishiwata, S. and Yoshida, M. (1998) Cell 93, 21–24.
[4] Boyer, P.D. (1997) Annu. Rev. Biochem. 66, 717–749.
[5] Junge, W., Lill, H. and Engelbrecht, S. (1997) Trends Biochem. Sci. 22, 420–423.
[6] Dimroth, P. (2000) Biochim. Biophys. Acta 1458, 374–386.
[7] Gupte, S.S., Chazotte, B., Leesnitzer, M.A. and Hackenbrock, C.R. (1991) Biochim. Biophys. Acta 1069, 131–138.
[8] Sabbert, D., Engelbrecht, S. and Junge, W. (1997) Proc. Natl. Acad. Sci. USA 94, 4401–4405.
[9] Abrahams, J.P., Leslie, A.G.W., Lutter, R. and Walker, J.E. (1994) Nature 370, 621–628.
[10] Weber, J. and Senior, A.E. (1996) J. Biol. Chem. 271, 3474–3477.
[11] Sabbert, D. and Junge, W. (1997) Proc. Natl. Acad. Sci. USA 94, 2312–2317.
[12] Sabbert, D., Engelbrecht, S. and Junge, W. (1997) Proc. Natl. Acad. Sci. USA 94, 4401–4405.
[13] Häsler, K., Engelbrecht, S. and Junge, W. (1998) FEBS Lett. 426, 301–304.
[14] Yasuda, R., Noji, H., Yoshida, M., Kinosita Jr., K. and Itoh, H. (2001) Nature 410, 898–904.
[15] Al-Shawi, M.K., Ketchum, C.J. and Nakamoto, R.K. (1997) J. Biol. Chem. 272, 2300–2306.
[16] Yasuda, R., Noji, H., Kinosita, K. and Yoshida, M. (1998) Cell 93, 1117–1124.
[17] Jones, P.C. and Fillingame, R.H. (1998) J. Biol. Chem. 273, 29701–29705.
[18] van Walraven, H.S., Strotmann, H., Schwarz, O. and Rumberg, B. (1996) FEBS Lett. 379, 309–313.
[19] Pänke, O. and Rumberg, B. (1997) Biochim. Biophys. Acta 1322, 183–194.
[20] Berry, S. and Rumberg, B. (1996) Biochim. Biophys. Acta 1276, 51–56.
[21] Stock, D., Leslie, A.G. and Walker, J.E. (1999) Science 286, 1700–1705.
[22] Seelert, H., Poetsch, A., Dencher, N.A., Engel, A., Stahlberg, H. and Mueller, D.J. (2000) Nature 405, 418–419.
[23] Stahlberg, H., Muller, D.J., Suda, K., Fotiadis, D., Engel, A., Meier, T., Matthey, U. and Dimroth, P. (2001) EMBO Rep. 2, 229–233.
[24] Junge, W., Lill, H. and Engelbrecht, S. (1997) Trends Biochem. Sci. 22, 420–423.
[25] Elston, T., Wang, H. and Oster, G. (1998) Nature 391, 510–514.
[26] Dimroth, P. (2000) Biochim. Biophys. Acta 1458, 374–386.
[27] Junge, W. (1999) Proc. Natl. Acad. Sci. USA 96, 4735–4737.
[28] Lill, H., Burkovski, A., Altendorf, K., Junge, W. and Engelbrecht, S. (1993) Biochim. Biophys. Acta 1144, 278–284.
[29] Burkovski, A., Lill, H. and Engelbrecht, S. (1994) Biochim. Biophys. Acta 1186, 243–246.
[30] Steinemann, D., Lill, H., Junge, W. and Engelbrecht, S. (1994) Biochim. Biophys. Acta 1187, 354–359.
[31] Häsler, K., Pänke, O. and Junge, W. (1999) Biochemistry 38, 13759–13765.
[32] Kaim, G. and Dimroth, P. (1995) Eur. J. Biochem. 218, 937–944.
[33] Kaim, G. and Dimroth, P. (1995) Eur. J. Biochem. 222, 615–623.
[34] Engelbrecht, S. and Junge, W. (1997) FEBS Lett. 414, 485–491.
[35] Dunn, S.D., McLachlin, D.T. and Revington, M. (2000) Biochim. Biophys. Acta 1458, 356–363.
[36] Heinz, D.W., Baase, W.A., Dahlquist, F.W. and Matthews, B.W. (1993) Nature 361, 561–564.
[37] Sorgen, P.L., Caviston, T.L., Perry, R.C. and Cain, B.D. (1998) J. Biol. Chem. 273, 27873–27878.

[38] Duncan, T.M., Bulygin, V.V., Zhou, Y., Hutcheon, M.L. and Cross, R.L. (1995) Proc. Natl. Acad. Sci. USA 92, 10964–10968.
[39] Iwamoto, A., Miki, J., Maeda, M. and Futai, M. (1990) J. Biol. Chem. 265, 5043–5048.
[40] Masaike, T., Mitome, N., Noji, H., Muneyuki, E., Yasuda, R., Kinosita, K. and Yoshida, M. (2000) J. Exp. Biol. Pt 1 203, 1–8.
[41] Jones, P.C., Hermolin, J. and Fillingame, R.H. (2000) J. Biol. Chem. 275, 11355–11360.
[42] Noji, H., Yasuda, R., Yoshida, M. and Kinosita, K. (1997) Nature 386, 299–302.
[43] Sabbert, D., Engelbrecht, S. and Junge, W. (1996) Nature 381, 623–626.
[44] Tsunoda, S.P., Aggeler, R., Yoshida, M. and Capaldi, R.A. (2001) Proc. Natl. Acad. Sci. USA 98, 898–902.
[45] Sambongi, Y., Iko, Y., Tanabe, M., Omote, H., Iwamoto-Kihara, A., Ueda, I., Yanagida, T., Wada, Y. and Futai, M. (1999) Science 286, 1722–1724.
[46] Noji, H., Yasuda, R., Yoshida, M. and Kinosita, K. (1997) Nature 386, 299–302.
[47] Tsunoda, S.P., Aggeler, R., Noji, H., Kinosita, K., Yoshida, M. and Capaldi, R.A. (2000) FEBS Lett. 470, 244–248.
[48] Böttcher, B. (2000) EMBO Rep. 1, 223–224.
[49] Pänke, O., Gumbiowski, K., Junge, W. and Engelbrecht, S. (2000) FEBS Lett. 472, 34–38.
[50] Kuo, P.H., Ketchum, C.J. and Nakamoto, R.K. (1998) FEBS Lett. 426, 217–220.
[51] Noji, H., Häsler, K., Junge, W., Kinosita Jr., K., Yoshida, M. and Engelbrecht, S. (1999) Biochem. Biophys. Res. Commun. 260, 597–599.
[52] Fillingame, R.H., Peters, L.K., White, L.K., Mosher, M.E. and Paule, C.R. (1984) J. Bacteriol. 158, 1078–1083.
[53] Tanabe, M., Nishio, K., Iko, Y., Sambongi, Y., Iwamoto-Kihara, A., Wada, Y. and Futai, M. (2001) J. Biol. Chem. 276, 15269–15274.
[54] Pänke, O., Gumbiowski, K., Junge, W. and Engelbrecht, S. (2000) FEBS Lett. 472, 34–38.
[55] Yasuda, R., Noji, H., Kinosita, K., Motojima, F. and Yoshida, M. (1997) J. Bioenerg. Biomembr. 29, 207–209.
[56] Sambongi, Y., Iko, Y., Tanabe, M., Omote, H., Iwamoto-Kihara, A., Ueda, I., Yanagida, T., Wada, Y. and Futai, M. (1999) Science 286, 1722–1724.
[57] Cherepanov, D.A. and Junge, W. (2001) Biophys. J. 81 (3), in press.
[58] Berg, H.C. (1993) Random Walks in Biology, Princeton University Press, Princeton, NJ.
[59] Hunt, A.J., Gittes, F. and Howard, J. (1994) Biophys. J. 67, 766–781.
[60] Pänke, O., Cherepanov, D.A., Gumbiowski, K., Engelbrecht, S. and Junge, W. (2001) Biophys. J. 81 (3), in press.
[61] Wang, H.Y. and Oster, G. (1998) Nature 396, 279–282.
[62] Kinosita Jr., K., Yasuda, R., Noji, H. and Adachi, K. (2000) Philos. Trans. R. Soc. Lond. B Biol. Sci. 355, 473–489.
[63] Gittes, F., Mickey, B., Nettleton, J. and Howard, J. (1993) J. Cell Biol. 120, 923–934.
[64] Isambert, H., Venier, P., Maggs, A.C., Fattoum, A., Kassab, R., Pantaloni, D. and Carlier, M.F. (1995) J. Biol. Chem. 270, 11437–11444.
[65] Tsuda, Y., Yasutake, H., Ishijima, A. and Yanagida, T. (1996) Proc. Natl. Acad. Sci. USA 93, 12937–12942.
[66] Yasuda, R., Miyata, H. and Kinosita Jr., K. (1996) J. Mol. Biol. 263, 227–236.
[67] Yasuda, R., Noji, H., Kinosita, K. and Yoshida, M. (1998) Cell 93, 1117–1124.
[68] Omote, H., Sambonmatsu, N., Saito, K., Sambongi, Y., Iwamoto-Kihara, A., Yanagida, T., Wada, Y. and Futai, M. (1999) Proc. Natl. Acad. Sci. USA 96, 7780–7784.
[69] Hisabori, T., Kondoh, A. and Yoshida, M. (1999) FEBS Lett. 463, 35–38.